Slug Void Fraction in Vertical Downward Gas-Liquid Two-Phase Flow

Faiza Saidj[1], Abderraouf Arabi[2], Hiba Bouyahiaoui[1], Abdelwahid Azzi[1*], Abbas H Hasan[3]

[1] LTPMP/FGMGP, Université des Sciences et de la Technologie Houari Boumediène, B.P 32 El Alia, Bab Ezzouar, Algiers 16111, Algeria

[2] Departament d'Enginyeria Mecànica, Universitat Rovira i Virgili, Av. Països Catalans 26, 43007, Tarragona, Spain

3 University of Hull, School of Engineering, HU6 7RX, UK

*Corresponding author: Abdelwahid Azzi, E-mail: aazzi@usthb.dz Tel: +(213) 771 45 89 26

Abstract

An accurate prediction of the liquid holdup and pressure drop using the one-dimensional mechanistic slug flow models requires an accurate estimation of slug void fraction. Considerable theoretical and experimental research has been conducted in literature to study the slug void fraction. However, almost, all these studies primarily focus on the vertical upward and horizontal slug flows. In this study, we investigated experimentally and theoretically the slug void fraction in vertical downward flow. A series of experiments for measuring the slug void fraction in air-water flow using the conductance probe technique with a pipe diameter of 34 mm were conducted. The relationship between the measured slug void fraction and the mixture velocity revealed the presence of three distinct zones. This observed behavior, which differs from what has been reported in vertical upward flow, was explained through a mechanistic model that considers the varying velocities of liquid slugs, small gas bubbles, and Taylor bubbles. A new empirical predictive model based on the liquid-to-gas superficial velocities ratio and input liquid fraction was proposed. The performance of the proposed model was compared to existing models and demonstrated the lowest error. It showed a good performance with an average relative error of -3.43% and an average absolute relative error of 12.97%. The assessment study of the existing models developed for vertical upward flow showed that they failed to predict correctly the slug void fraction in vertical downward flow.

Keywords: gas-liquid flow; vertical downward flow; slug flow; slug void fraction; mechanistic model; conductance technique.

Nomenclature

A	Empirical coefficient	[-]
C	Empirical coefficient	[-]
C_O	Distribution coefficient	[-]
D	Pipe diameter	[m]
Ge^*	Dimensionless conductance	[-]
Fr_M	Mixture Froude number	[-]
f_s	Slug friction factor	[-]
L_{eb}	Elongated bubble length	[m]
L_s	Slug length	[m]
L_{su}	Slug unit length	[m]
N_μ	Viscosity number	[-]
Re_M	Mixture Reynolds number	[-]
U_{gs}	Gas superficial velocity	[m/s]
U_{ls}	Liquid superficial velocity	[m/s]
V_b	Gas bubbles velocity	[m/s]
V_{gd}	Drift velocity	[m/s]
V_M	Mixture velocity	[m/s]
V_{full}	Voltage for pipe filled with liquid	[V]
V_{out}	Output voltage	[V]
V_s	Slug velocity	[m/s]
Vt	Translational velocity	[m/s]
ε_g	Global void fraction	[-]
ε_{geb}	Elongated bubble void fraction	[-]
ε_{gs}	Slug void fraction	[-]
θ	Pipe inclination	[°]
λ_l	Input liquid fraction	[-]
μ_l	Liquid viscosity	[Pa.s]
ρ_g	Gas density	[kg/m^3]
ρl	Liquid density	[kg/m^3]
σ	Surface tension	[N/m]

1 Introduction

Intermittent flow, also known as slug flow (Arabi et al., 2025), is a complex flow regime commonly found in variety of energetic systems such as hydrocarbon production and transportation, airlift pumping systems, power generation systems, CO_2 capture and storage, nuclear power plants, and chemical processing industries (Zhang et al., 2018; Bordalo et al., 2024; Holagh and Ahmed, 2024; Tiselj et al., 2024; Du et al., 2024). In this flow regime, the two phases align themselves as two flow structures which flow alternatively: elongated bubble and liquid slug (Höhn et al., 2024). A couple of elongated bubble and liquid slug forms a unit cell. In the horizontal and inclined pipes, the elongated bubbles flows over a liquid film; while the liquid film starts belting the elongated bubbles when the pipe inclination increases positively or decrease negatively. The liquid slugs carry out generally small gas bubbles.

The mechanistic models, introduced in the 70's, are considered as the most reliable way for modeling the hydrodynamic parameters (Arabi et al., 2024), notably the pressure drop and void fraction. The mechanistic approach is based on applying one dimensional continuity and momentum conservation equations for each phase. The robustness of this approach lies on that it considers the nature of the flow regimes. In fact, the continuity and conservation equations are applied by considering the nature of the interfaces. For slug flow, the averaged void fraction on the slug unit (ε_g) can be calculated by (Sylvester, 1987):

$$\varepsilon_g = \frac{L_s}{L_{su}}\varepsilon_{gs} + \frac{L_{eb}}{L_{su}}\varepsilon_{geb} \tag{1}$$

where ε_{gs}, ε_{geb}, L_s, L_{eb} and L_{su} refer respectively to the slug void fraction, elongated bubble void fraction, slug length, elongated bubble length and slug unit length. Generally, the elongated bubble void fraction is calculated from the simultaneous resolution of continuity and momentum equations; while the slug void fraction is calculated using predictive models that are used as input parameter.

Accurately estimating the input parameters is essential for the performance of predictions made by mechanistic models (Arabi et al., 2024). Thus, it is important to correctly predicting the slug void fraction. Since the pioneering work performed by Gregory et al. (1978). Several experimental works were carried out to generate the experimental databases for vertical slug flow (Felizola, 1992; Al-Ruhaimani, 2015; Saidj et al., 2018; Abdul-Majeed and Al-Mashat, 2019). The slug void fraction is generally determined by processing the void fraction time series measured by the conductance technique (Höhn et al., 2024). The conductance probes demonstrated their competitiveness in the sense that they are no-intrusive, relatively cheap, simple in design and showed a fast-response (Shi et al., 2020; Ghendour et al., 2020). In addition, the outputs given by this technique are found in agreement with those obtained using more advanced techniques such as wire mesh sensor technique (Abdulkadir et al., 2019).

From a phenomenological point of view, Brauner and Ullmann (2004) attributed the slug aeration to a recurrent bubble entrainment from the Taylor bubble tail and their re-coalescence at the successive Taylor bubble. Based on this explanation, they developed a mechanistic model for predicting the slug aeration level for horizontal, vertical and inclined upward flow. A summary of the main theoretical and empirical models for predicting slug void fraction is presented in Table 1. For more details about these models, see for example Abdul-Majeed et al. (2022) and Soto-Cortes et al. (2024). Note that the slug void fraction models can also be used to predict the flow transition mechanism, e.g. bubbly to slug, slug to churn or plug to slug flows (Barnea and Brauner, 1985; Hasan et al., 2019; Boutaghane et al., 2023).

Table 1. Summary of the existing models to predict ε_{gs}.

Authors and year	**Model**
Gregory et al. (1978)	$\varepsilon_{gs} = 1 - \dfrac{1}{1 + \left(\dfrac{V_M}{8.66}\right)^{1.39}}$
Barnea and Brauner (1985)	$\varepsilon_{gs} = 0.058\left[2\left(\dfrac{0.4\,\sigma}{(\rho_l - \rho_g)g}\right)^{1/2}\left(\dfrac{2\ f_s {V_M}^3}{D}\right)^{2/5}\left(\dfrac{\rho_l}{\sigma}\right)^{3/5} - 0.725\right]^2$
	$f_s = 0.046{Re_M}^{-0.2}$
	$Re_M = \dfrac{\rho_l\, D\, V_M}{\mu_l}$
Sylvester (1987)	$\varepsilon_{gs} = \dfrac{U_{gs}}{0.425 + 2.65V_M}$
Gomez et al. (2000)	$\varepsilon_{gs} = 1 - 1.0\ e^{-(0.00784\ \theta + 2.48\ 10^{-6}\ Re_M)}$
Abdul-Majeed (2000)	$\varepsilon_{gs} = 1 - (1 - C\ V_M)\ A$
	$C = 0.06 + 1.3377\left(\dfrac{\mu_g}{\mu_l}\right)$
	$A = 1$ if $\theta \leq 0$ $A = 1 - sin\theta$ if $\theta > 0$

Abdul-Majeed and Al-Mashat (2019)	$\varepsilon_{gs} = 0.016 - 0.000611\,\theta - (0.000124\,\theta - 0.0195) Fr_M {N_\mu}^{-0.2}$
	$Fr_M = \sqrt{\frac{\rho_l}{\rho_l - \rho_g}} \frac{V_M}{\sqrt{gD}}$
	$N_\mu = \frac{V_M \mu_l}{g D^2 (\rho_l - \rho_g)}$
Maldonado et al. (2024)	$\varepsilon_{gs} = 3.87 \left(\frac{U_{gs}}{U_{ls}}\right)^{0.012} + 0.034 Re_M^{0.22} - 4.056$
Al-Sarkhi et al. (2024)	$\varepsilon_{gs} = 1 - \frac{\lambda_l}{1.03635 + \left(\frac{-1.03235}{1 + \left(\frac{U_{ls}}{0.912922 U_{gs}}\right)^{1.00557}}\right)}$
	$\lambda_l = \frac{U_{ls}}{V_M}$

An analysis of the models presented in Table 1 shows that the majority of them recourse to the mixture velocity (V_M), given by Eq. 2, indicating that the slug void fraction is significantly influenced by the mixture velocity (Abdul-Majeed and Firouzi, 2019). Using the database collected from previous studies, Al-Sarkhi et al. (2024) reported that the slug void fraction can be correlated by the liquid-to-gas superficial velocities (U_{ls}/U_{gs}) and the input liquid fraction (λ_l) which is also referred to homogenous liquid fraction. By using these two dimensionless numbers, the collected data by Al-Sarkhi et al. (2024) was perfectly aligned to cover a wide range of fluids, pipe diameters, and pipe inclinations. One advantage of the Al-Sarkhi et al. model, in comparison to other slug flow models, is its ability to capture the impact of U_{ls}/U_{gs} and λ_l on the slug void fraction, as explained in Al-Sarkhi and Fdleseed (2024).

$$V_M = U_{gs} + U_{ls} \tag{2}$$

$$\lambda_l = \frac{U_{ls}}{V_M} \tag{3}$$

Almost, all the predictive slug liquid holdup models currently available in literature were developed and validated for horizontal, vertical and inclined flows. Additionally, to the best of the authors' knowledge, there is currently no publicly available experimental database of slug void fraction obtained for vertical downward flows.

Bhagwat and Ghajar (2012) studied the similarity and differences of the global void fraction and the flow patterns in upward and downward two-phase flow. They reported that the void fraction in vertical upward flow is always less than that in the downward flow. They showed that when the drift flux model with negative drift velocity is used for downward flows, the percentage error between the predicted void fraction and measured void fraction is within ±20%.

Usui and Sato (1989) who studied and visualized the vertical downward air-water two-phase flow reported that most of the gas slugs in downward flow do not have the bullet shape seen in upward flow. Instead, they are distorted with a wedge shape and a small curved end. Additionally, the frothy wake formed at the leading lower end is caused by the liquid flowing down the surrounding gas slug. Therefore, bubbles are found to flow down in an oscillating and sometimes spiral motion along the wall. This mechanism could cause the values of the distribution coefficient and gas drift velocity, in the drift flux model, to vary between downward slug flow and upward slug flow.

The physical mechanism and the existing correlations of vertical upward slug flow configuration (where the inertia and gravity acts on opposite direction) cannot be applied and generalized to the vertical downward slug flow (where the gravitational force acts on the direction of the flow). This in turn, highlight the need to study the physical mechanism of vertical downward slug flow and identify different flow parameters such as the slug void fraction through theoretical and experimental studies. In addition, there is a lack in the literature of mechanistic models for vertical downward two-phase flow, as stated in the recent review by Ali et al. (2024) and others. Downward vertical flows can be found in many industries and applications. In the context of oil and gas depletion and energy transition, there is an increase utilization of Microbial Enhanced Oil Recovery (MEOR), the plate-type nuclear fuel of research reactors and CO_2 capture and storage, in which the vertical downward gas-liquid slug flow can be encountered (Bouyahiaoui et al., 2024). This interest induces the necessity to advance in the mechanistic modeling as well as in the improving of the performance of closure models.

The aim of this study was to address the lack of slug void fraction data by generating an experimental database of slug void fraction for vertical downward two-phase flow. The experiments were done for air-water mixture and a 34 mm internal diameter pipe. A new simple mechanistic model was developed for slug void fraction in vertical downward two-phase flow and compared to other existing models.

2 Experimental facility

The experiments were conducted using the experimental apparatus established and used by Saidj et al. (2018); Ghendour et al. (2021), Zeghloul et al. (2021); Bouyahiaoui et al. (2024). This apparatus has the capability to capture the time series of flow parameters, such as void fraction and pressure drop, of gas-liquid two-phase flow in various flow regimes, including vertical and downward slug flow. For this study, the experiments were carried out with the vertical downward configuration. Details about this configuration can be found in Bouyahiaoui et al. (2018; 2020). The experimental setup is depicted in Figure 1. The pipe test section, which is made of Perspex to enable visualization, measures 7.8 m in length and has an internal diameter of 34 mm. Air supplied by a compressor and water provided by a pump, are mixed in the inlet mixer section. The resulting two-phase flow initially moves through a vertical pipe segment of about one meter, through an inverted 180° bend before flowing vertically downward in the vertical test section.

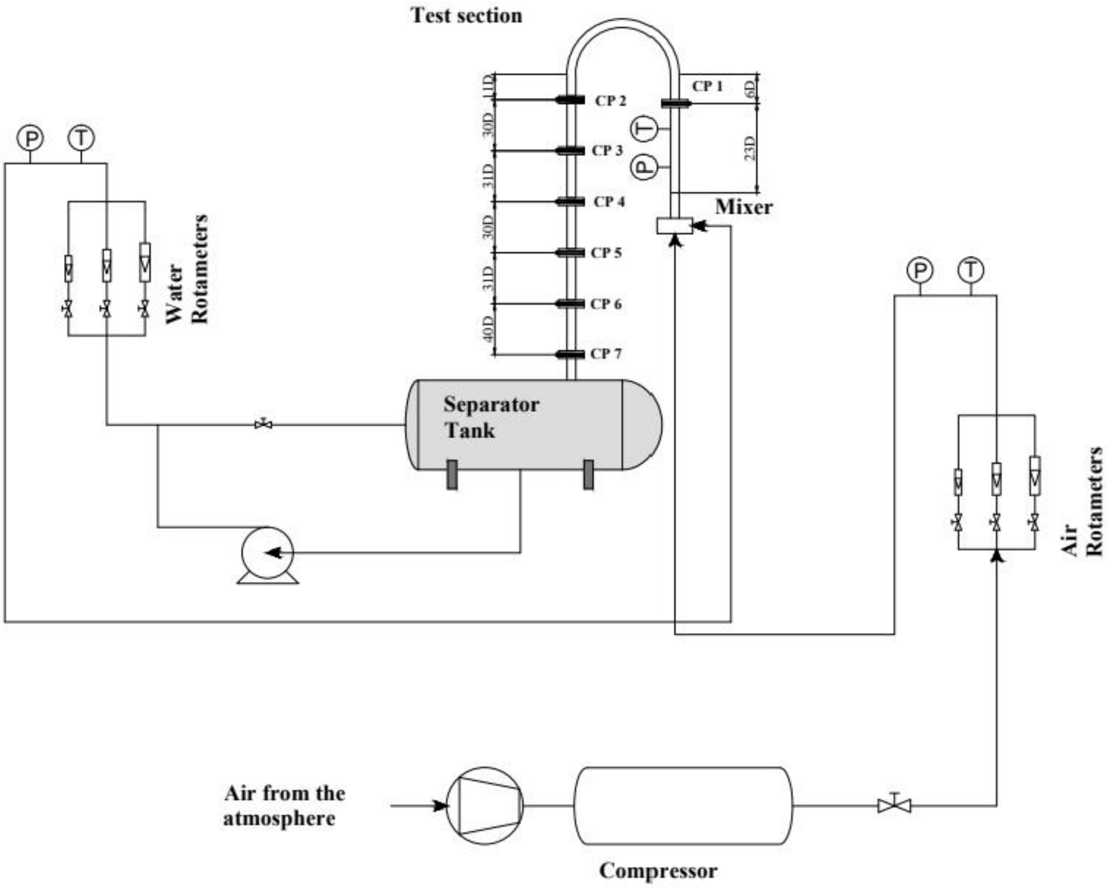

Figure 1. Schematic diagram of experimental setup.

A series of acquisition of void fraction time series was carried out using the conductance technique. The conductance technique is a well-established method for measuring void fraction in horizontal and vertical two-phase flows (Coney, 1973; Fossa et al. (1998), Zhao et al. (2016), Zeghloul et al., 2020; Hasan et al., 2021). Seven conductance probes (CP), CP1 to CP7 are installed in this flow test facility. The first probe, CP1, is positioned 6 pipe diameters upstream the inverted U-bend and the CP2 to CP7 probes are installed at 11, 41, 72, 102, 134 and 173 pipe diameters, respectively.

It should be noted that the void fraction in the current study was obtained from CP7 to ensure a fully developed slug flow. This was also confirmed by the time series data as well as visual observations.

A conductance probe technique developed at our laboratory was employed to measure the void fraction, leveraging the conductive properties of water and the resistive characteristics of air. This method enables the determination of the cross-sectional averaged void fraction by establishing a correlation between the electrical impedance of the medium and the phase distribution.

The probe generates an output voltage (V_{out}) that is directly related to the resistance of the air-water mixture. This response is then transformed into a dimensionless conductance (Ge^{*}) by referencing the voltage measured when the pipe is completely filled with liquid (V_{full}).

To account for changes in water resistance, V_{full} was measured prior to each experimental run and adjusted if significant drift was detected. The calibration process involved generating various liquid fractions over the conductance probes by placing plastic plugs and beads in the pipe, simulating annular and bubbly flow conditions, respectively.

Figure 2 presents the calibration curve relating the dimensionless conductance ($Ge*$) to the void fraction. This curve, represented by a third-order polynomial, aligns well with the theoretical model proposed by Tsochatzidis et al. (1992). The theoretical curve is derived from the analytical solution of the Laplace equation, which describes the behavior of the electrodes. A comprehensive analysis of the derivation of this equation can be found in the work conducted by Tsochatzidis et al. (1992).

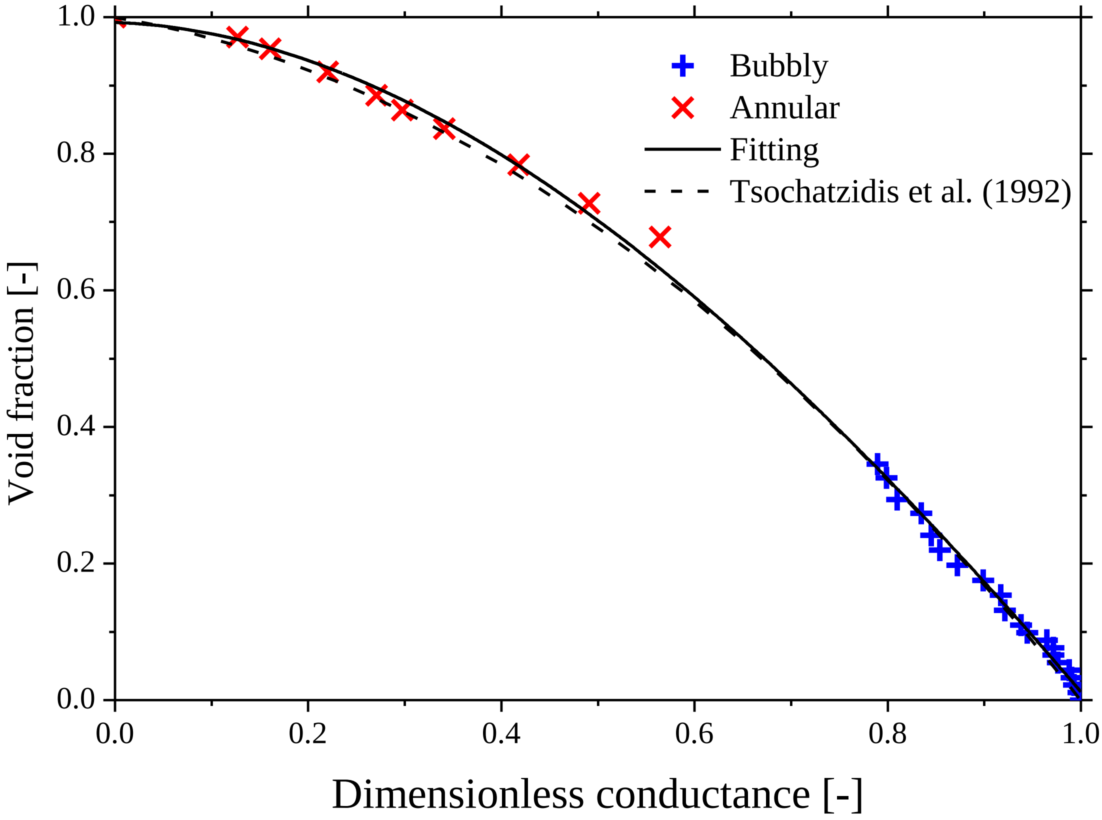

Figure 2. Calibration curve of the conductance probe and its comparison with the theoretical model proposed by Tsochatzidis et al. (1992).

The LabView 8.6 software, combined with a 12-bit NI DAQ card (6062E), was utilized to record the time responses of each conductance probe. Data were collected over a 60-second interval at a sampling frequency of 200 Hz.

3 Results

The main focus of this paper was on fully developed slug flow. Therefore, 38 experimental data sets were extracted using the last conductance probe CP7. The mixture velocity was in the range of 0.57 and 1.67 m/s. In this range of superficial velocities, a slug flow regime was observed (Fig. 3).

Figure. 3. A photo of slug regime obtained for U_{ls}=0.58 m/s and U_{gs}=0.23 m/s.

It can be seen from this figure that similarly to the upward slug flow, the vertical downward slug flow is characterized by the intermittent flow of the long-elongated gas bubbles called Taylor bubble followed by a bridge of liquid filled by small gas bubbles. The Taylor bubble diameter is comparable to that of the pipe.

What is important to note is that the Taylor bubble has its nose oriented upward, opposite to the flow direction, which is downward. Additionally, the tip of the nose of this Taylor bubble is off-centred and shifted toward the tube wall. This can be attributed to the effect of the liquid phase's weight on the gas phase.

The experimental conditions are represented in the flow map of Qiao et al. (2017), see Fig.4. It should be mentioned that these data points were also confirmed through visual observations of the transparent downward vertical pipe flow.

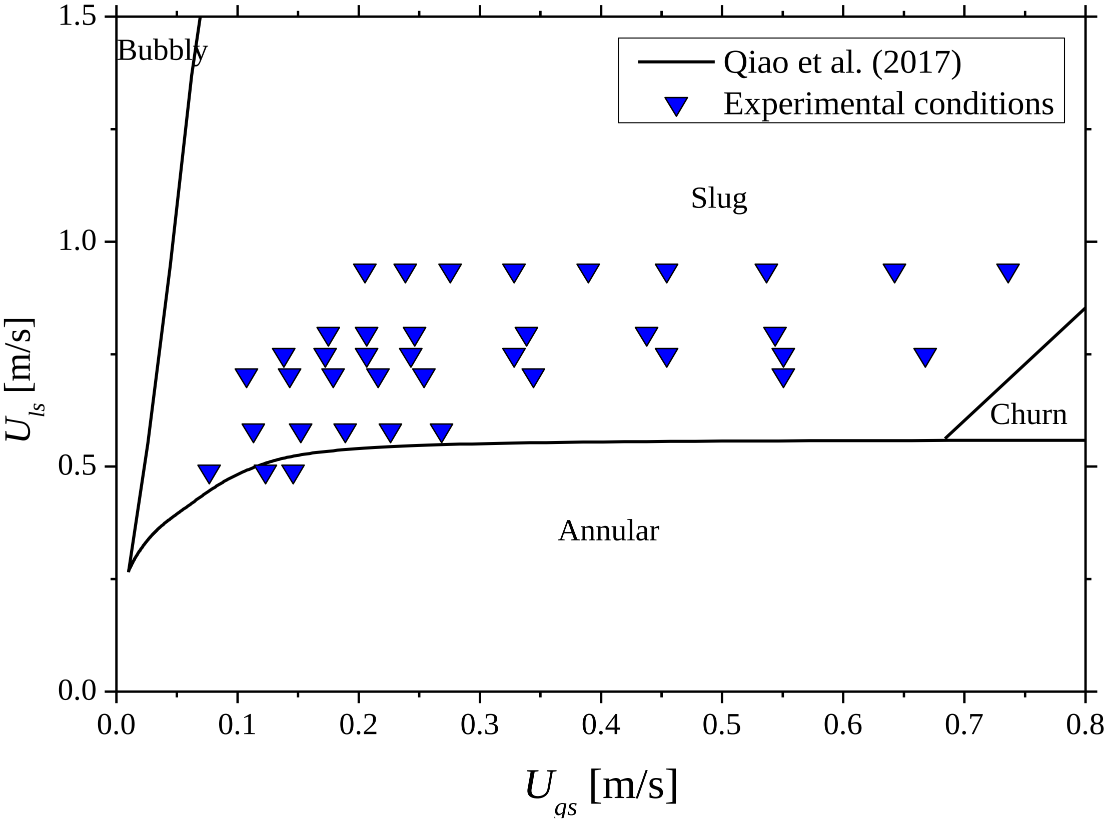

Figure 4. Representation of experimental condition in the flow map of Qiao et al. (2017).

Figure 5.a shows an example of void fraction time series signals collected for U_{ls} = 0.58 m/s and U_{gs} = 0.15 m/s. The signal is composed of clear peaks separated by valleys zones. The peaks and valleys correspond respectively to the passage of elongated bubble and liquid slugs through the senor. This time series found is a typical shape of the slug flow (Bouyahiaoui et al., 2024). The obtained Probability Density Function (PDF) from this signal, represented in Fig. 5.b, displays the presence of two distinct peaks. The peaks occurring at higher and lower values of void fraction corresponds to the void fraction inside the Taylor bubble region and liquid slugs. Similar technique was notably used in our previous work carried out for vertical upward two-phase flow (Saidj et al., 2018).

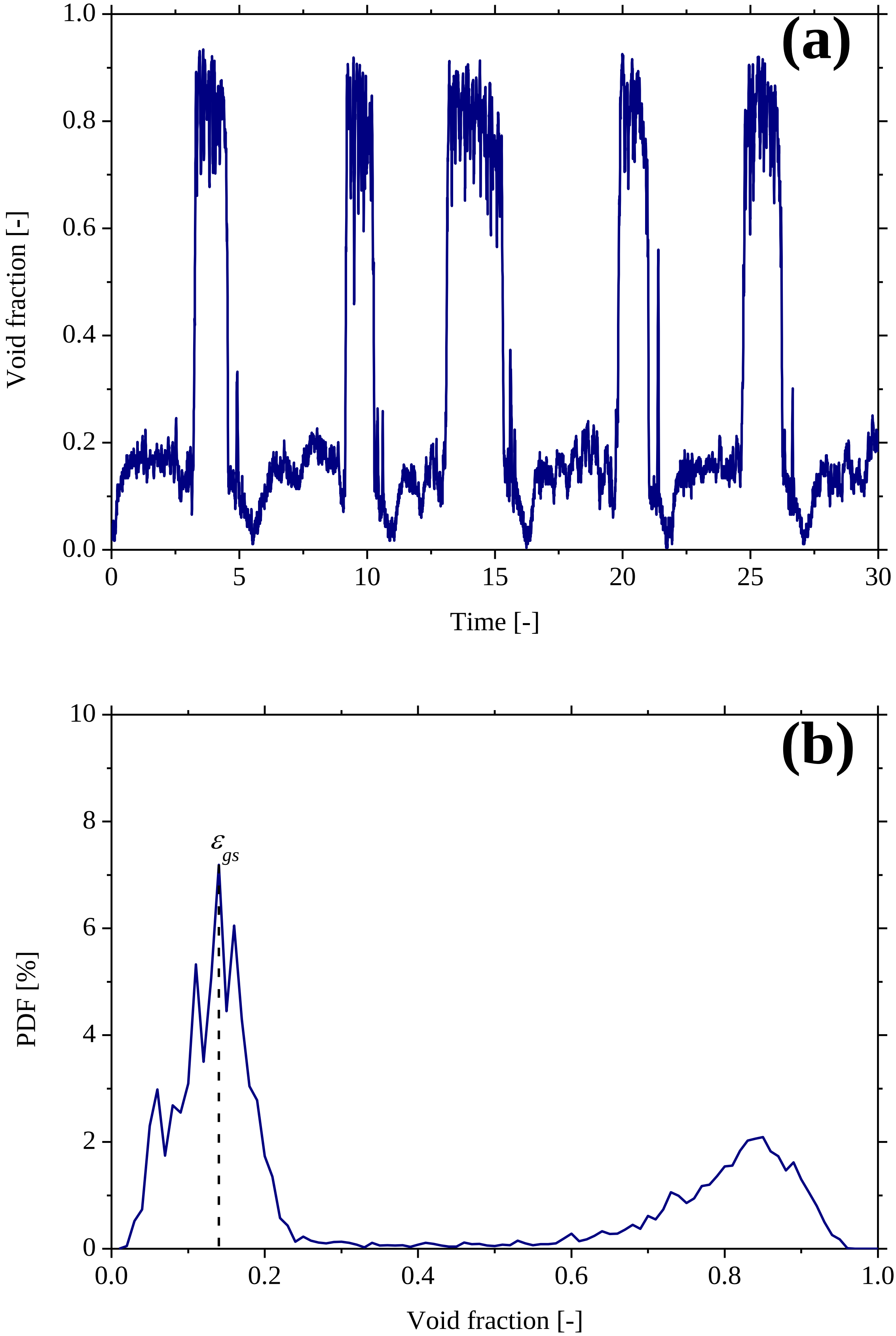

Figure 5. Example of obtained void fraction signal and PDF

The variation of the void fraction as a function of the mixture velocity is plotted in Fig. 6.a. The relationship between void fraction and mixture velocity is not straightforward but shows different tendencies. To analyze this further, the obtained results are represented as a function of the liquid supercritical velocity as shown in Fig. 6.b. This allows to see the effect of different liquid supercritical velocities on the void fraction trends. Fig. 6.b showed three distinct zones. In zone 1, the increase of mixture velocity induces a decrease of slug void fraction. The transition between zones 1 and 2, which occurs at $V_M \approx 0.92$ m/s, results in an increase in the slug aeration level and a chaotic variation of the slug void fraction before stabilizing in zone 3. For V_M superior to ~ 1.05 m/s, it appears that the slug void fraction becomes independent to the mixture velocity.

To compare the variation of the void fraction in downward flows and upward flows, the void fraction data obtained by Saidj et al. (2018) who investigated the gas-liquid vertical upward flow is presented in Fig. 6.c. Note that the same experimental setup, conductance sensor and pipe diameter are employed in both studies. Comparing Fig. 6.a with Fig. 6.c, one can see that the range or the span of the slug void fraction in vertical upward flow seems to be more than that in the downward flows. Additionally, unlike the downward flow, the increase of the mixture velocity in the vertical upward flow causes a general increase in the slug void fraction. As explained in Section 1, this behavior is well established in the literature for horizontal, vertical upward and inclined two-phase flow.

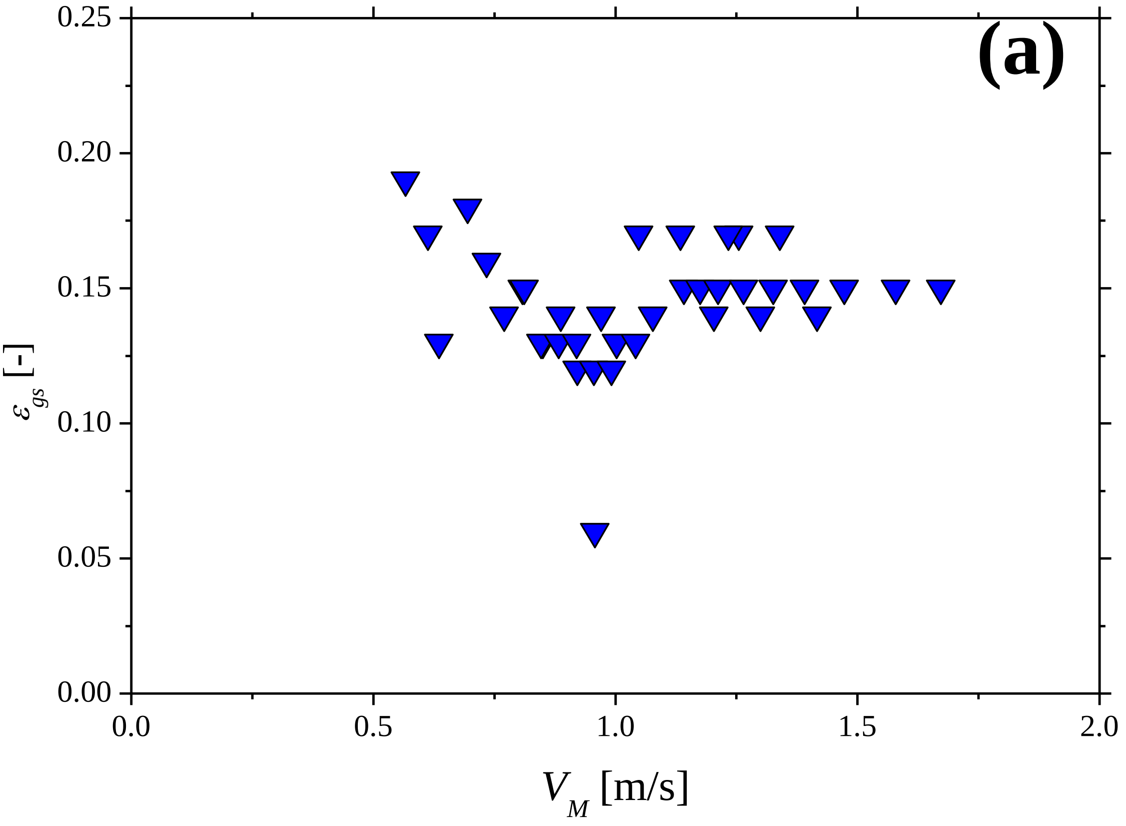
(a)
ε_{gs} [-]
0.25
0.20
0.15
0.10
0.05
0.00
0.0
0.5
1.0
1.5
2.0
V_M [m/s]

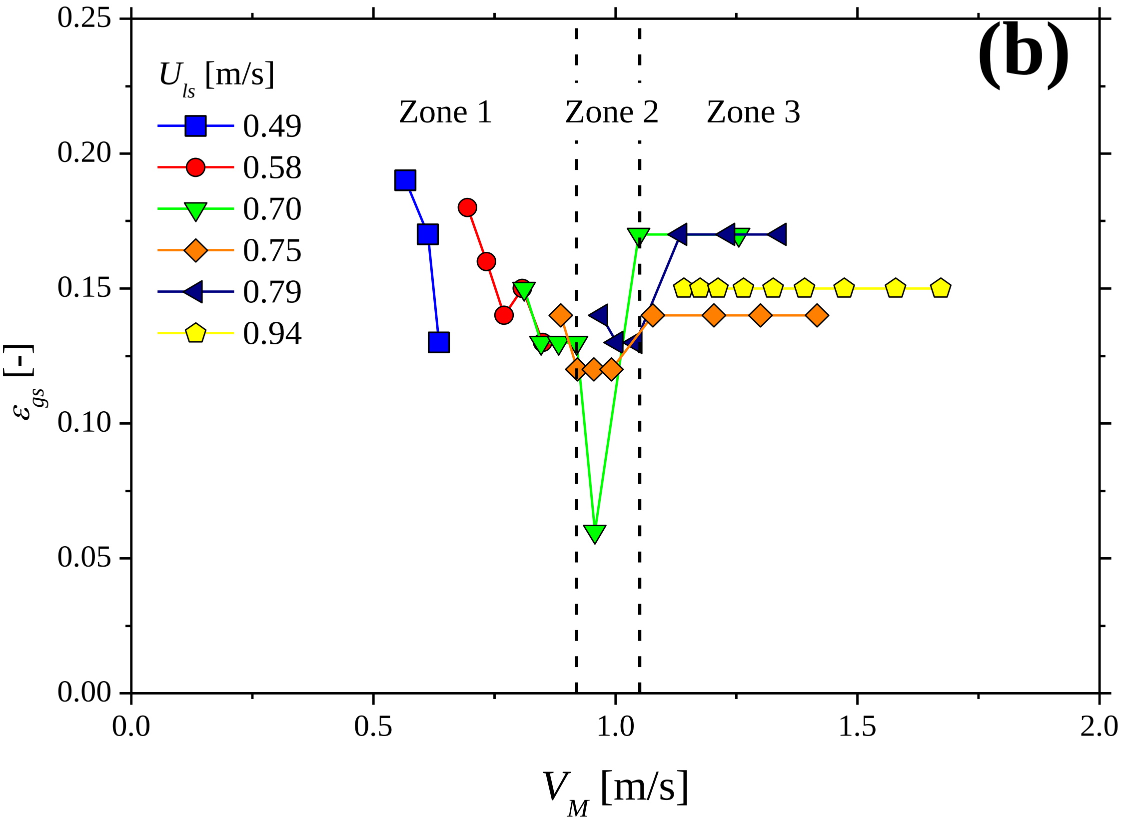
(b)
U_{ls} [m/s]
0.49
0.58
0.70
0.75
0.79
0.94
Zone 1
Zone 2
Zone 3
ε_{gs} [-]
0.25
0.20
0.15
0.10
0.05
0.00
0.0
0.5
1.0
1.5
2.0
V_M [m/s]

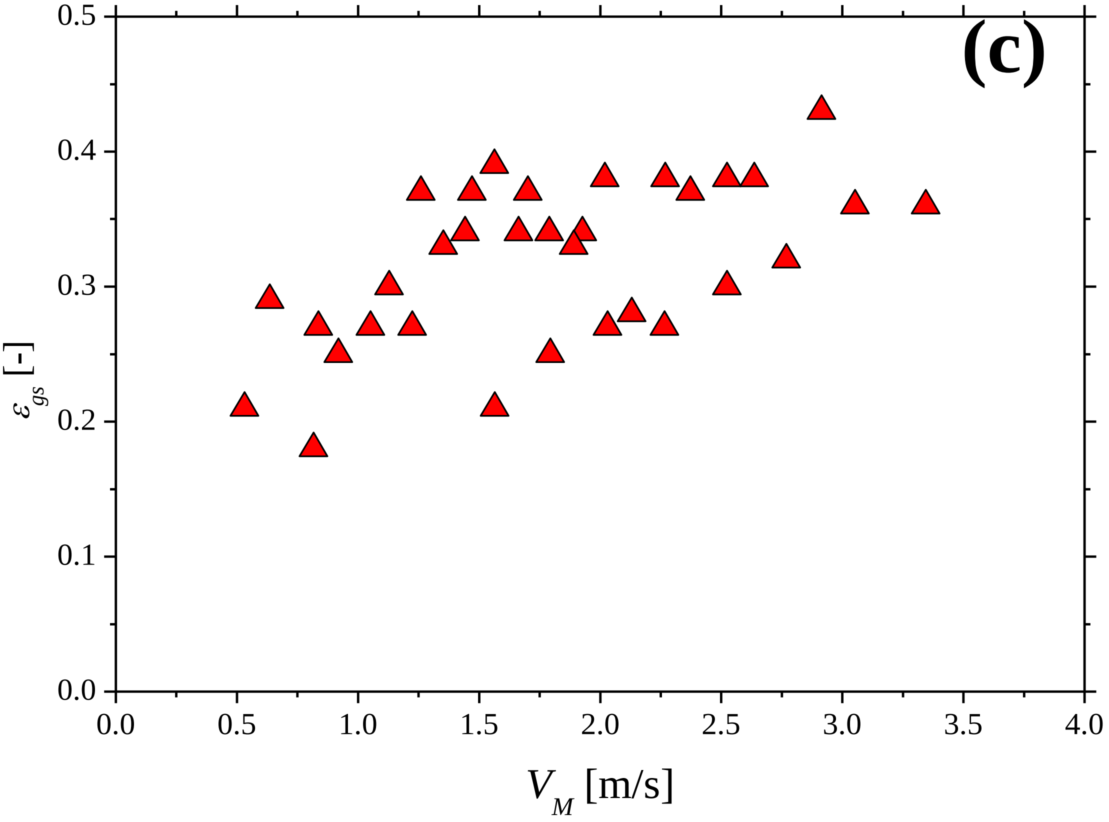

Figure 6. Plot of measured ε_{gs} as a function of V_M (a) present study; (b) present study with highlighting the effect of U_{ls}; and (c) obtained by Saidj et al. (2018) for vertical upward case;

The liquid slug void fraction was plotted as a function of gas-to-liquid superficial velocities ratio and input liquid fraction λ_l (Al-Sarkhi and Fdleseed, 2024). The results are displayed in Fig. 7.a and Fig.7.b, respectively. Similar tendencies observed in Fig. 6.a are obtained.

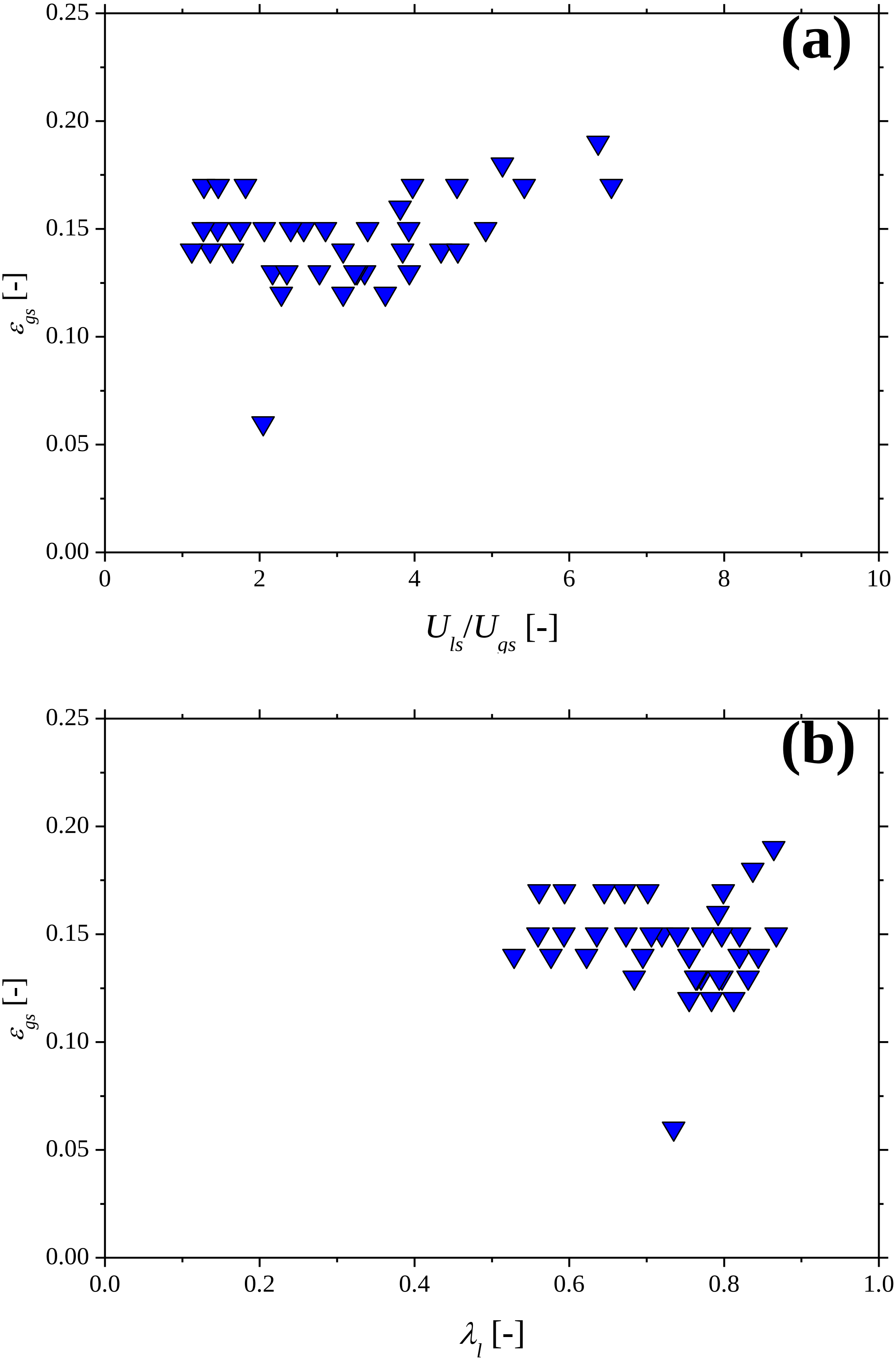

Figure 7. Plot of the measured ε_{gs} as a function of (a) U_{sl}/U_{sg} and (b) λ_l.

4 Discussions

The slug aeration process is a complex phenomenon resulting from the simultaneous occurrence of several physical interactions, such as turbulence, differences in velocities between elongated bubbles and liquid slugs, bubble fragmentation, and entrapment. (Brauner and Ullmann, 2004; Issa et al., 2006). In horizontal pipes, the slug aeration is due to the interfacial shear induced waves, shearing-off and shearing scooping of bubbles mechanisms which are related to the nature of the sub-regimes (Arabi et al., 2025). For vertical and inclined upward configuration, Soto-Cortes et al. (2024) reported that due to the buoyancy, the gas bubbles within liquid slugs moves upward at lower velocity than the liquid slug which induces an increase of void fraction. In vertical downward flow, the flow is composed of a series of elongated bubbles flowing between liquid slugs, as shown in Fig. 8. At developed region, the liquid slug flows at a constant velocity (V_s) which is approximately equal to V_M (Brauner and Ullmann, 2004; Dong et al., 2021); while the velocity of Taylor bubble is referred to translational velocity V_t.

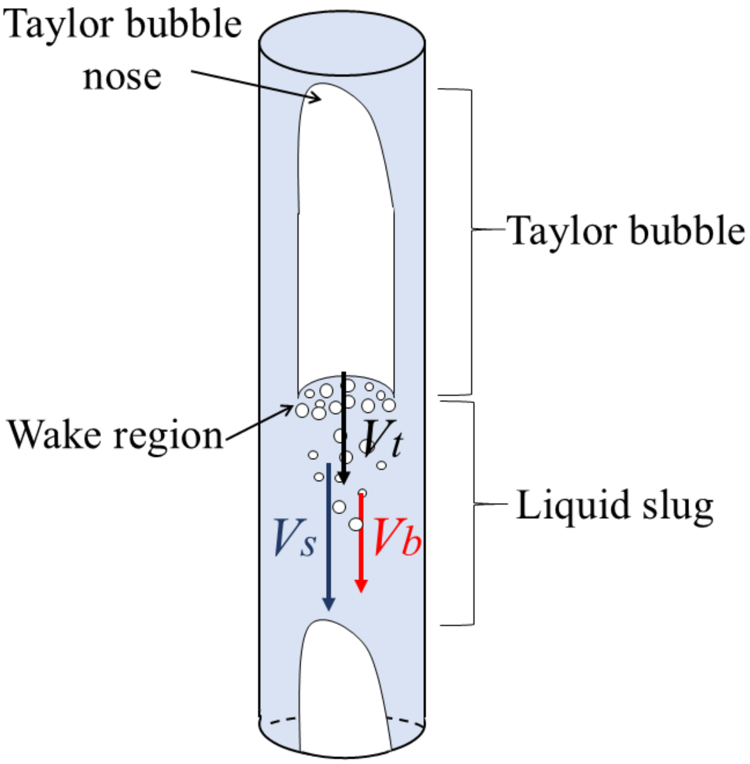

Figure 8. Schematic diagram of a slug unit for vertical downward two-phase flow.

In contrary to vertical upward and horizontal flow, the translational velocity in downward flows is generally less than the mixture velocity, as it can be seen in Fig. 9 when we plot together the curves given by the correlations of Nicklin et al. (1962) developed for vertical upward flow and the one of Bouyahiaoui et al. (2018) obtained from measurement carried out on vertical downward flow. Note that the behavior seen with the correlation of Bouyahiaoui et al. (2018) is also visible with the findings reported in Martin (1976).

In downward flow, the fact that the buoyancy acts on the opposite direction to the flow induces a negative value of the drift velocity (which is the intersect of the correlations). The fact that the distribution coefficient (the slope of the correlations) is lower than the unity is due to the shape of the elongated bubble which has an asymmetrical nose in vertical downward flow (Usui and Sato, 1989; Lu and Prosperetti, 2006; Fershtman et al., 2017; Lizarraga-Garcia et al., 2021, Tiselj et al., 2024; Kren et al., 2024).

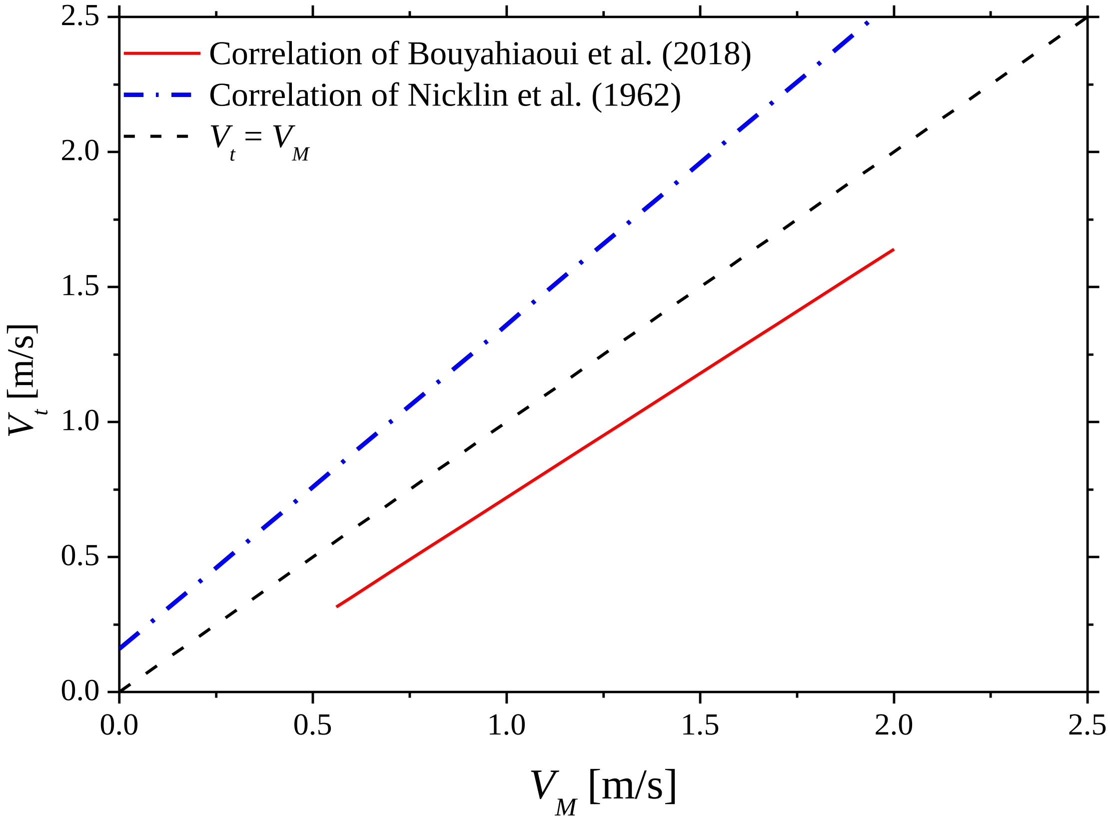

Figure 9. Plot of V_t calculated using the correlation of Bouyahiaoui et al. (2018) and Nicklin et al. (1962) as function of V_M.

It is seen from Fig. 9 that in vertical downward flow, and in contrary to vertical upward flow, the Taylor bubble flows with lower velocity than the following liquid slug. As a consequence, there is a discharge of a liquid, forming a liquid film around the Taylor bubble. The contact of the liquid film, which flows at higher velocity than V_t, with the tail of Taylor bubble results in the formation of a plunging jet which can generate the recirculation zones behind the Taylor bubbles. This in turn, induces the shear of gas bubbles from the Taylor bubble, generating the wake region at the tail of Taylor bubbles. Intuitively, the energy of the jet depends notably on the velocity difference between Taylor bubble and liquid slugs. The detached gas bubbles created will flow within liquid slugs at a velocity V_b. Due to the buoyancy force, which tends to slow down the flow of bubbles, V_b becomes lower than V_s. In other words, the gas bubbles in the liquid slug behave like a dispersed bubbly flow (Brauner and Ullmann, 2004). The bubble velocity in the liquid slug, V_b can be calculated using the drift flux model (Eq. 4). By employing the correlation of Goda et al. (2003), the distribution parameter (C_0) and the drift velocity (V_{gd}) are calculated using Eq. 5 and Eq. 6. Note that the choice of this correlation was motivated by (i) it was developed specifically for vertical downward two-phase flow by using a large database, and (ii) a large number of data used are obtained with bubbly flow.

$$V_g = C_0 V_M + V_{gd} \tag{4}$$

$$C_0 = \begin{cases} \left(0.772 + 0.0214 \dfrac{V_M}{\sqrt{2}\left(\frac{g\sigma(\rho_L - \rho_G)}{\rho_L^2}\right)^{0.25}}\right) + \left(0.228 - 0.0214 \dfrac{V_M}{\sqrt{2}\left(\frac{g\sigma(\rho_L - \rho_G)}{\rho_L^2}\right)^{0.25}}\right)\sqrt{\dfrac{\rho_G}{\rho_L}} \text{ for } \dfrac{V_M}{\left(\frac{g\sigma(\rho_L - \rho_G)}{\rho_L^2}\right)^{0.25}} \leq 20 \\ \left(1.0 + 0.2exp\left(0.0848\left(20 - \dfrac{V_M}{\sqrt{2}\left(\frac{g\sigma(\rho_L - \rho_G)}{\rho_L^2}\right)^{0.25}}\right)\right)\right) - 0.2exp\left(0.0848\left(20 - \dfrac{V_M}{\sqrt{2}\left(\frac{g\sigma(\rho_L - \rho_G)}{\rho_L^2}\right)^{0.25}}\right)\right)\sqrt{\dfrac{\rho_G}{\rho_L}} \text{ for } \dfrac{V_M}{\left(\frac{g\sigma(\rho_L - \rho_G)}{\rho_L^2}\right)^{0.25}} > 20 \end{cases} \tag{5}$$

$$V_{gd} = -\sqrt{2}\left(\frac{g\sigma(\rho_L - \rho_G)}{\rho_L^2}\right)^{0.25} \tag{6}$$

The slip velocity between the liquid slug and the gas bubbles (V_s-V_b) as well as between the Taylor bubble and the gas bubbles (V_t-V_b) are calculated and represented as function of V_M in Fig. 10. The Taylor bubble translational velocity was computed using the correlation of Bouyahiaoui et al. (2018). A close observation of the two curves shown in Fig. 10 reveals the presence of three distinct zones, this can also be observed from the three different slopes. At V_M = 1.225 m/s, the curve of V_s-V_b passes from an increase to a decrease tendency. This change in tendency separates the zones 1 and 2. On the other hand, the zone 3 starts when $V_t - V_b \leq 0$. In Zone 1 (at lower mixture velocity, $V_M \leq 1.225$ m/s), the velocity of the small bubbles in the liquid slug V_b move much slower than the liquid slug V_s with the increment of the mixture velocity, causing an increase in the slip velocity (V_s- V_b). Thus, the gas bubbles in the liquid slug are delayed, allowing them to be caught by the following Taylor bubbles, which could lead to the reduction in ε_{gs}. This also aligns with the previous observation found in Fig. 6.a and Fig. 6.b. In zone 2, an increase of mixture velocity provokes a decrease of the difference between the liquid slugs and the dispersed bubbles, which as upward vertical configuration, leads to an increase of liquid slug aeration level (Soto-Cortès et al., 2024). From $V_M \geq 1.749$ m/s, announcing the beginning of zone 3, V_b starts to be more important than V_t, thus the gas bubbles catch the previous Taylor bubbles. The coalescence occurs at the Taylor bubble nose. This phenomenon is possible according to the experimental observations reported by Fabre and Figueroa-Espinoza (2014).

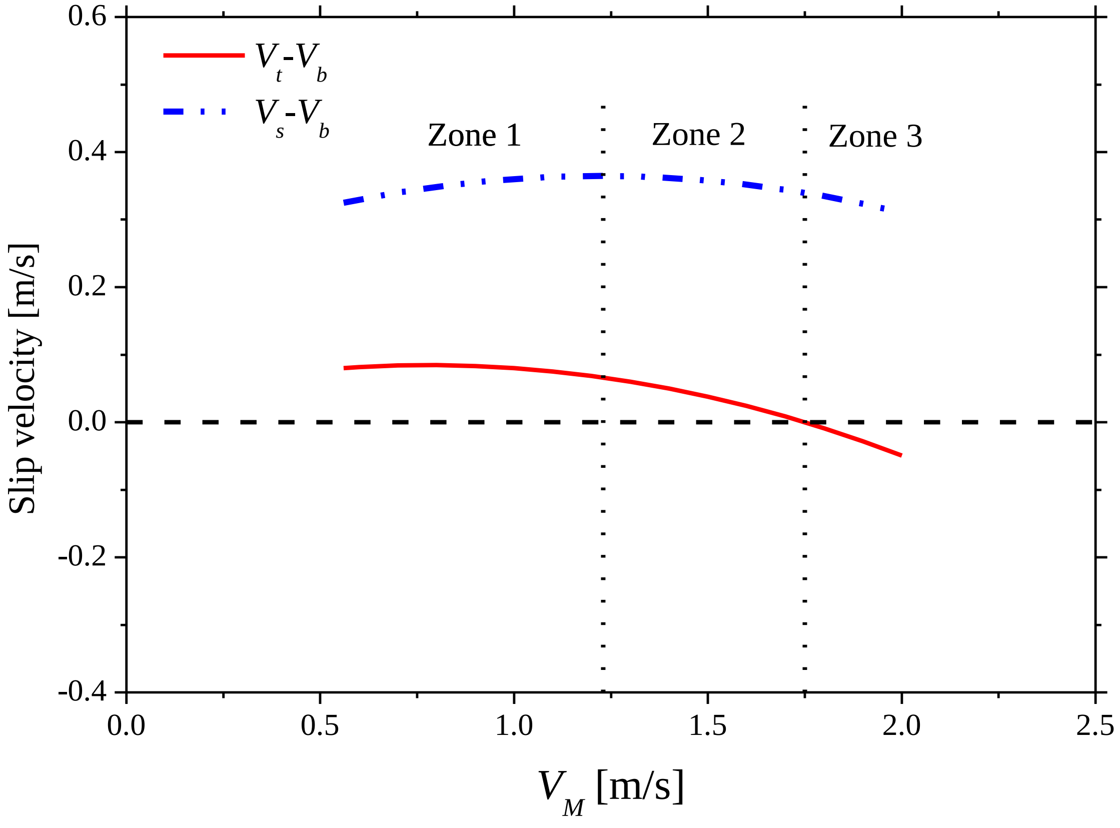

Figure 10. Evolution of slip velocities V_t-V_b and V_s-V_b as function of V_M.

A comparison between Fig. 10 and Fig. 6.b shows that the values of V_M corresponding to the transition between the zones 1 and 2 are relatively close (0.92 m/s and 1.225 m/s, which represent a deviation of 33%). However, the critical mixture velocity that separates zones 2 and 3 (as shown in Fig. 10 and Fig. 6.b) has been determined with a significant difference of 66.5%. The fact that the final slug void fraction values in the zone 3 depends only on the liquid superficial velocities, as shown in Fig.6.b, suggests the presence of an additional mechanism, in addition to the slip velocities between the Taylor bubble translational velocity and the gas bubbles, responsible for the generation of the bubbles. Further experimental investigations should be conducted to gain a better understanding of the slug aeration mechanism occurring in zone 3. The presented explanations using a simple mechanistic model have to be considered as a first attempt to explain qualitatively the reported behavior of slug void fraction for this flow configuration. Further experimental works using local measurements are strongly encouraged by the authors to confirm the presented interpretations. These measurements will also help pave the way for the development of a mechanistic model to simulate slug flow in vertical downward two-phase flow.

Following Al-Sarkhi et al. (2024) work, we represented in Fig. 11. the results of slug void fraction using the the ratio $\lambda_l/(1-\varepsilon_{gs})$ as a function of U_{ls}/U_{gs}. By fitting the data (see Fig. 11), the parameters a, b and c in (Eq.7) were determined to be 2.0767, -0.4649, and -0.4287, respectively. The summary of the regression statistics and the statistical data of the three empirical coefficients are summarized in Table 2 and Table 3, respectively. The formula of the proposed correlation is given in Eq. 8.

$$\frac{\lambda_L}{1-\varepsilon_{gs}} = \left(\frac{a}{1+\left(\frac{U_{ls}}{U_{gs}}\right)^{b}} \right) + c \tag{7}$$

$$\varepsilon_{gs} = 1 - \frac{\lambda_L}{\left(\frac{2.0767}{1+\left(\frac{U_{ls}}{U_{gs}}\right)^{-0.4649}} \right) - 0.4287} \tag{8}$$

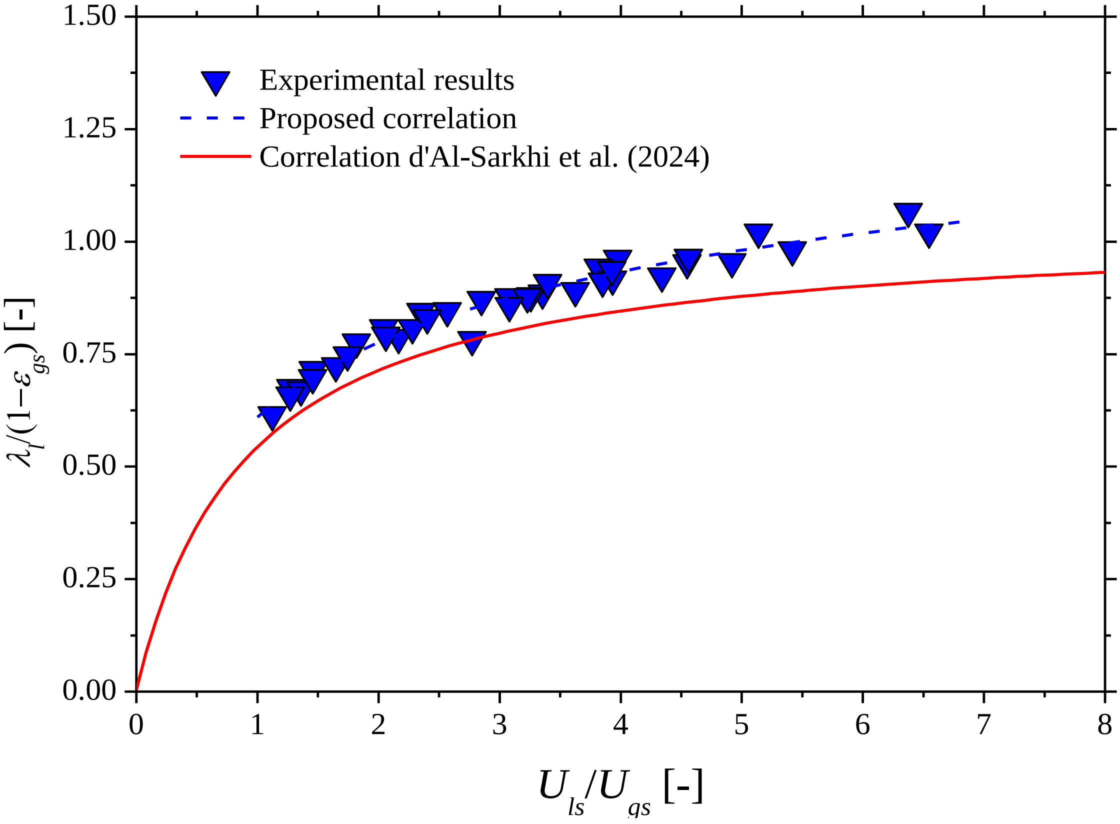

Figure 11. Plot of the measured ε_{gs} using $\lambda_l/(1-\varepsilon_{gs})$ as function of U_{ls}/U_{gs}.

Table 2. Regression statistic of the proposed correlation

Parameters	Value
SSE	0.0161
R-square	0.9644
DFE	35.0000
Adj R-sqr	0.9623
RMSE	0.0215

Table 3. Statistical data (value and 95% confidence bounds) of the empirical coefficients of the developed correlation.

Coefficient	Value	Lower	Upper
a	2.0767	-0.3771	4.5304
b	-0.4649	-1.0834	0.1535
c	-0.4282	-1.6389	0.7815

The simultaneous plot of the proposed equation and the correlation of Al-Sarkhi et al. (2024) $\lambda_l/(1\text{-}\varepsilon_{gs})$ as function of U_{ls}/U_{gs} in Fig. 11 allows to see that $\lambda_l/(1\text{-}\varepsilon_{gs})$ exhibits higher values in vertical downward flow comparatively to horizontal, vertical upward and inclined flows.

The predictions given by the existing slug void fraction models, summarized in Table 1, as well as the proposed one were compared with the obtained measurements. For each model, the deviation between the experimental measurements and the predictions were quantified using the average relative error (*ARE*) and the absolute average relative error (*AARE*), given by Eq. 9 and Eq. 10, respectively

$$ARE = \sum_{i=1}^{N} \frac{\varepsilon_{gs,cal} - \varepsilon_{gs,meas}}{\varepsilon_{gs,meas}} \tag{9}$$

$$AARE = \sum_{i=1}^{N} \left| \frac{\varepsilon_{gs,cal} - \varepsilon_{gs,meas}}{\varepsilon_{gs,meas}} \right| \tag{10}$$

where, N is the number of data sample. The subscripts *cal* and *meas* refer to calculated and measured values, respectively.

Table 4. Performance evaluation of the existing models and the proposed one.

Models	***ARE* (%)**	***AARE* (%)**
Gregory et al. (1978)	63.60	63.60
Barnea and Brauner (1985)	98.40	98.40
Sylvester (1987)	36.96	40.10
Abdul-Majeed (2000)	34.24	36.36
Maldonado et al. (2024)	18.67	29.13
Al-Sarkhi et al. (2024)	56.95	56.95
Present model	-3.43	12.97

By observing the values of parameters *ARE* and *AARE* summarized in Table 4, it appears that all the previous models overestimate largely the slug void fractions. The models of Gregory et al. (1978), Barnea and Brauner (1985) and Al-Sarkhi et al. (2024) all show a tendency to overestimate all the data points, where both *ARE* and *AARE* are equal. The proposed correlation presented in this paper (Eq. 8) gives the best results among other models, with *ARE* and *AARE* equal to -3.43% and 12.97%, respectively.

The cross plots of the experimental results and the predictions given by the existing slug void fraction models in the literature as well as the proposed correlation are presented in Fig.12. It is seen that the majority of the points deviate from the measurement with ±20%. Based on the assessment studies carried out in recent studies of Al-Sarkhi et al. (2024), Soto-Cortes et al. (2024) and Nwanwe et al. (2024), it appears that the developed correlation in the current study is reasonably accurate. However, additional validations are needed at a wide range of experimental conditions.

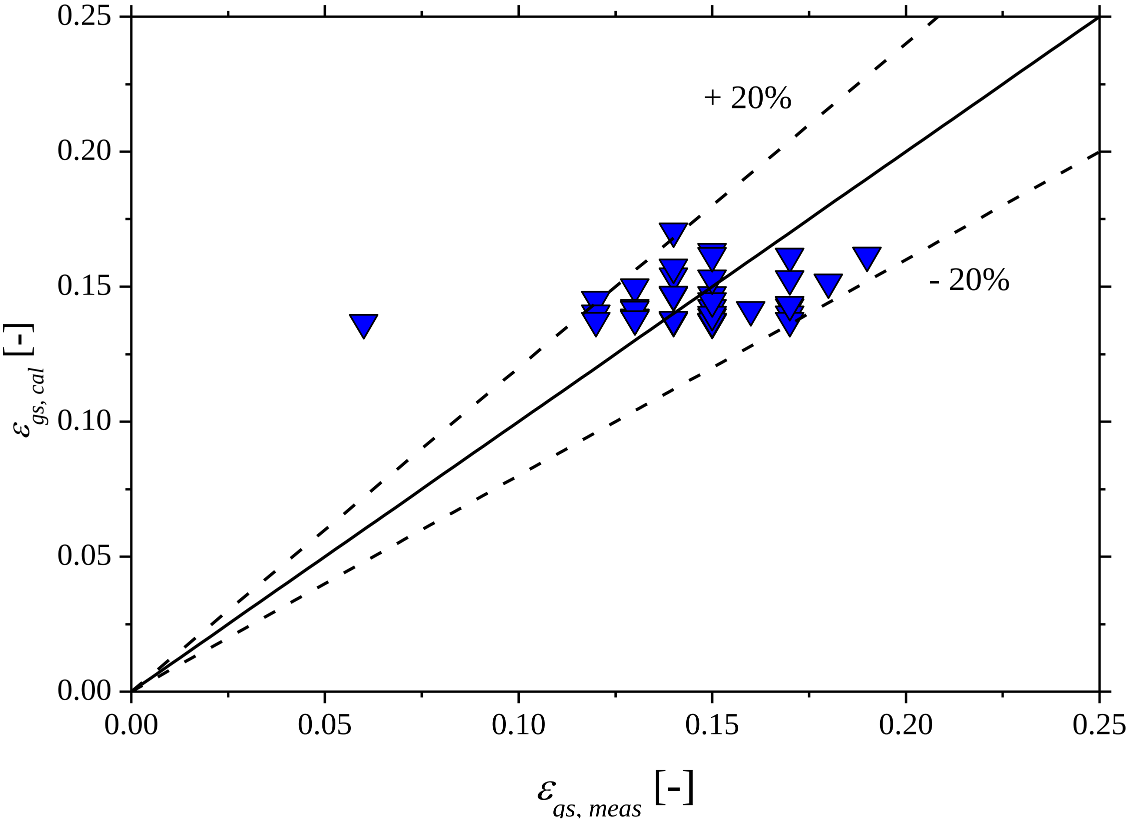

Figure 12. Cross plot of the measured and predicted ε_{gs} using the existing models and the proposed one.

5. Conclusions

In this paper, the experimental study was conducted to investigate the slug void fraction in vertical downward two-phase flows. The experimental data sets and the new empirical predictive model developed can be used to enhance understanding of the slug downward flow behavior in various industries including oil and gas, nuclear, carbon capture and storage, and the chemical industry. In addition, the experimental data presented in this study can be utilized by modellers to validate their CFD models in the vertical downward slug flow field. A summary of the key findings is outlined below:

- At low to moderate mixture velocity, the slug void fraction in vertical downward flow seems to be dependent on the mixture velocity. Three flow zones were observed. At low mixture velocity (zone 1), there was a significant decrease in the slug void fraction. In the transition zone of moderate mixture velocity (zone 2), there was a chaotic variation in the slug void fraction before it became independent of the mixture velocity (zone 3).
- When comparing the slug void fraction in downward flow with that in upward flow, it is observed that the range (or the span) of the slug void fraction in upward flow is greater. Additionally, the slug void fraction appears to be independent of the mixture velocity at lower value of the mixture velocity compared to upward flow.
- A simple mechanistic model was developed which shows that the slip velocities between the gas bubbles and liquid slug, and between the gas bubbles and Taylor bubble depend on the mixture velocity and might be the reason behind the existence of three flow zones.
- Using the dimensionless numbers: liquid-to-gas superficial velocities and input liquid fraction, a simple predictive correlation was proposed. This correlation was found to give better predictions than existing ones, with *ARE* and *AARE* less than ± 3.5% and 13%, respectively.

It is important to view this study as a first step to study, understand and correlate the slug void fraction for this specific pipe configuration. Thus, further experimental works are strongly encouraged to enrich the presented database, notably for other fluids and pipe diameters. Further detailed investigations using local measurements are also highly recommended to better explain the physical mechanisms of slug aeration for this flow configuration.

Acknowledgements

Dr. Abderraouf Arabi has received funding from the postdoctoral fellowships programme Beatriu de Pinós (2021 BP 00052), funded by the Secretary of Universities and Research (Government of Catalonia) and by the Horizon 2020 Programme of Research and Innovation of the European Union under the Marie Skłodowska-Curie grant agreement No. 801370.

References

Abdulkadir, M., Mbalisigwe, U. P., Zhao, D., Hernandez-Perez, V., Azzopardi, B. J., & Tahir, S. (2019). Characteristics of churn and annular flows in a large diameter vertical riser. International Journal of multiphase flow, 113, 250-263.

Abdul-Majeed, G. H. (2000). Liquid slug holdup in horizontal and slightly inclined two-phase slug flow. Journal of Petroleum Science and Engineering, 27(1-2), 27-32.

Abdul-Majeed, G. H., & Al-Mashat, A. M. (2019). A unified correlation for predicting slug liquid holdup in viscous two-phase flow for pipe inclination from horizontal to vertical. SN Applied Sciences, 1(1), 1-25.

Abdul-Majeed, G. H., & Firouzi, M. (2019). The suitability of the dimensionless terms used in correlating slug liquid holdup with flow parameters in viscous two-phase flows. International Communications in Heat and Mass Transfer, 108, 104323.

Abdul-Majeed, G. H., Kadhim, F. S., Almahdawi, F. H., Al-Dunainawi, Y., Arabi, A., & Al-Azzawi, W. K. (2022). Application of artificial neural network to predict slug liquid holdup. International Journal of Multiphase Flow, 150, 104004.

Ali, A. A., Abdul-Majeed, G. H., & Al-Sarkhi, A. (2024). Review of Multiphase Flow Models in the Petroleum Engineering: Classifications, Simulator Types, and Applications. Arabian Journal for Science and Engineering, 1-44.

Al-Ruhaimani, F. (2015). Experimental Analysis and Theoretical Modeling of High Liquid Viscosity Two-phase Upward Vertical Pipe Flow. Ph.D. Dissertation. The University of Tulsa, Tulsa, OK.

ALSARKHI, A., & FDLESEED, A. (2024). Unmasking the Mystery: The Path to Accurate Liquid Slug Holdup Prediction. Geoenergy Science and Engineering, 213331.

Alsarkhi, A., Sarica, C., & Pereyra, E. (2024). Novel correlations for the liquid holdup in a gas-liquid slug flow. Geoenergy Science and Engineering, 237, 212825.

Arabi, A., Höhn, R. L., Pallares, J. & Stiriba, Y. (2024). Practical Aspects of Multiphase Slug Frequency: An Overview. The Canadian Journal of Chemical Engineering (Article in Press).

Arabi, A., Zenati, Y., Legrand, J., & Si-Ahmed, E. K. (2025). Sub-regimes of horizontal gas–liquid intermittent flow: State-of-the-art and future challenges. Experimental Thermal and Fluid Science, 111281.

Archibong-Eso, A., Okeke, N. E., Baba, Y., Aliyu, A. M., Lao, L., & Yeung, H. (2019). Estimating slug liquid holdup in high viscosity oil-gas two-phase flow. Flow measurement and instrumentation, 65, 22-32.

Bhagwat, S. M., & Ghajar, A. J. (2012). Similarities and differences in the flow patterns and void fraction in vertical upward and downward two- phase flow. Experimental thermal and fluid science, 39, 213-227.

Bordalo, S. N., Morooka, C. K., & Trigo, C. C. (2024). An experimental study of oscillations induced by two-phase slug flows of water and air on a flexible catenary shaped submerged pipe. Geoenergy Science and Engineering, 239, 212866.

Boutaghane, A., Arabi, A., Ibrahim-Rassoul, N., Al-sarkhi, A., & Azzi, A. (2023). Analysis, Comparison, and Discussion on the Utilization of the Existing Slug Liquid Holdup Models to Predict the Horizontal Gas-Liquid Plug-to-Slug Flow Transition. Journal of Energy Resources Technology, 145(7), 074501.

Bouyahiaoui, H., Azzi, A., Zeghloul, A., Hasan, A. H., Al-Sarkhi, A., & Parsi, M. (2020). Vertical upward and downward churn flow: Similarities and differences. Journal of Natural Gas Science and Engineering, 73, 103080.

Bouyahiaoui, H., Azzi, A., Zeghloul, A., Hasan, A., & Berrouk, A. S. (2018). Experimental investigation of a vertically downward two-phase air-water slug flow. Journal of Petroleum Science and Engineering, 162, 12-21.

Bouyahiaoui, H., Saidj, F., Arabi, A., Al-Sarkhi, A., & Azzi, A. (2024). Vertically downward gas-liquid flow: Void fraction and pressure drop. International Journal of Multiphase Flow, 172, 104711.

Brauner, N., & Ullmann, A. (2004). Modelling of gas entrainment from Taylor bubbles. Part A: Slug flow. International Journal of Multiphase Flow, 30(3), 239-272.

Coney, M., (1973). The theory and application of conductance probes for the measurement of liquid film thickness in two-phase flow. Journal of Physics E: Scientific Instruments, 6(9), 903-910.

Fabre, J., & Figueroa-Espinoza, B. (2014). Taylor bubble rising in a vertical pipe against laminar or turbulent downward flow: symmetric to asymmetric shape transition. Journal of fluid mechanics, 755, 485-502.

Felizola, H. (1992). Slug Flow in Extended Reach Directional Wells. Msc. Thesis. The University of Tulsa, Tulsa, OK. USA.

Fershtman, A., Babin, V., Barnea, D., & Shemer, L. (2017). On shapes and motion of an elongated bubble in downward liquid pipe flow. Physics of Fluids, 29(11).

Dong, C., Qi, R., & Zhang, L. (2021). Flow and heat transfer for a two-phase slug flow in horizontal pipes: A mechanistic model. Physics of Fluids, 33(3).

Du, Y., Zhu, J., Han, X., Fu, M., Li, M., & Shen, Y. (2024). Gas state equation and flow mechanism of gas–liquid two-phase flow in airlift pump system. Physics of Fluids, 36(5).

Fossa, M. (1998). Design and performance of a conductance probe for measuring the liquid fraction in two-phase gas-liquid flows. Flow measurement and instrumentation, 9, 103-109.

Ghendour, N., Azzi, A., Meribout, M., & Zeghloul, A. (2021). Modeling and design of a new conductance probe for gas void fraction measurement of two-phase flow through annulus. Flow Measurement and Instrumentation, 82, 102078.

Ghendour, N., Meribout, M., & Azzi, A. (2020). Review of measurement techniques for void fraction of two-phase flow through annulus. Measurement, 165, 108196.

Goda, H., Hibiki, T., Kim, S., Ishii, M., & Uhle, J. (2003). Drift-flux model for downward two-phase flow. International journal of heat and mass transfer, 46(25), 4835-4844.

Gomez, L. E., Shoham, O., & Taitel, Y. (2000). Prediction of slug liquid holdup: horizontal to upward vertical flow. International journal of multiphase flow, 26(3), 517-521.

Gregory, G. A., Nicholson, M. K., & Aziz, K. (1978). Correlation of the liquid volume fraction in the slug for horizontal gas-liquid slug flow. International Journal of Multiphase Flow, 4(1), 33-39.

Hasan, A.H., Shara K. Mohammed, Laura Pioli, Buddhika N. Hewakandamby, Barry J. Azzopardi (2019). Gas rising through a large diameter column of very viscous liquid: Flow patterns and their dynamic characteristics. International Journal of Multiphase Flow, 116, 1-14.

Hasan, A.H., Shara K. Mohammed, Hewakandamby, B., Azzopardi, B. (2021). Experimental study of the three-dimensional interfacial wave structure of freely falling liquid film in a vertical large pipe diameter. Chemical Engineering Research and Design, 169, 66-76.

Höhn, R. L., Arabi, A., Stiriba, Y., & Pallares, J. (2024). A Review of the Measurement of the Multiphase Slug Frequency. Processes, 12(11), 2500.

Holagh, S. G., & Ahmed, W. H. (2024). Critical review of vertical gas-liquid slug flow: An insight to better understand flow hydrodynamics' effect on heat and mass transfer characteristics. International Journal of Heat and Mass Transfer, 225, 125422.

Issa, R. I., Bonizzi, M., & Barbeau, S. (2006). Improved closure models for gas entrainment and interfacial shear for slug flow modelling in horizontal pipes. International Journal of Multiphase Flow, 32(10-11), 1287-1293.

Kren, J., Frederix, E. M. A., Tiselj, I., & Mikuž, B. (2024). Numerical study of Taylor bubble breakup in counter-current flow using large eddy simulation. Physics of Fluids, 36(2).

Lizarraga-Garcia, E., Buongiorno, J., & Al-Safran, E. (2021). Computational fluid dynamics (CFD) simulations of Taylor bubbles in vertical and inclined pipes with upward and downward liquid flow. SPE Journal, 26(06), 3832-3847.

Lu, X. and Prosperetti, A. (2006). Axial stability of Taylor bubbles. Journal of Fluid Mechanics, 568:173–192.

Maldonado, P. A., Rodrigues, C. C., Mancilla, E., dos Santos, E. N., da Fonseca Junior, R., Neto, M. A. M., da Silva, J. M. & Morales, R. E. (2024). Spatial Distribution of Void Fraction in the Liquid Slug in Vertical Gas-Liquid Slug Flow. Experimental Thermal and Fluid Science, 111093.Mohammadi, S.,

Martin, C. S. (1976). Vertically downward two-phase slug flow. Journal of Fluids Engineering, 98(4): 715-722.

Qiao, S., Mena, D., & Kim, S. (2017). Inlet effects on vertical-downward air–water two-phase flow. Nuclear Engineering and Design, 312, 375-388.

Nicklin, D. J. (1962). Two-phase flow in vertical tube. Trans. Instn. Chem. Engrs., 40, 61-68.

Nwanwe, C. C., Duru, U. I., Anyadiegwu, C. I. C., Ekejuba, A. I., Onwukwe, S. I., Nwachukwu, A. N., & Okonkwo, B. U. (2024). An artificial neural network visible mathematical model for predicting slug liquid holdup in low to high viscosity multiphase flow for horizontal to vertical pipes. Journal of Engineering and Applied Science, 71(1), 194.

Saidj, F., Hasan, A., Bouyahiaoui, H., Zeghloul, A., & Azzi, A. (2018). Experimental study of the characteristics of an upward two-phase slug flow in a vertical pipe. Progress in Nuclear Energy, 108, 428-437.

Shi, X., Tan, C., Dong, F., dos Santos, E. N., & da Silva, M. J. (2020). Conductance sensors for multiphase flow measurement: A review. IEEE Sensors journal, 21(11), 12913-12925.

Soto-Cortes, G., Pereyra, E., & Sarica, C. (2024). Unified closure relationship for slug liquid holdup. The Canadian Journal of Chemical Engineering. (Article in press).

Sylvester, N. D. (1987). A Mechanistic Model for Two-Phase Vertical Slug Flow in Pipes. Journal of Energy Resources Technology, 109(4), 206.

Tiselj, I., Kren, J., Mikuž, B., Nop, R., Burlot, A., & Hamrit, G. (2024). Experimental and numerical study of Taylor bubble in counter-current turbulent flow. Arabian Journal for Science and Engineering, 1-18.

Tsochatzidis,N., Karapantsios,T., Kostoglou, M., Karabelas, A. (1992). A conductance probe for measuring liquid fraction in pipes and packed beds. International Journal of Multiphase Flow 18, 653–667.

Usui, K., Sato, K. (1989). Vertically Downward Two-Phase Flow, (I). Journal of Nuclear Science and Technology, 26(7), 670-680.

Zhao, D., Omar, R., Abdulkadir, M., Abdulkareem, L.A., Azzi, A., Saidj F., Hernandez Perez V., Hewakandamby, N.B, Azzopardi, B.J. (2017). The control and maintenance of desired flow patterns in bends of different orientations. Flow measurement and instrumentation, 53, 230-242.

Zhang, W., Shao, D., Yan, Y., Liu, S., & Wang, T. (2018). Experimental investigations into the transient behaviours of CO2 in a horizontal pipeline during flexible CCS operations. International Journal of Greenhouse Gas Control, 79, 193-199.

Zeghloul, A., Abdelkader Messilem, Nabil Ghendour, Abdelsalam Al-Sarkhi, Abdelwahid Azzi, Hasan, A. (2020). Proceedings of the Institution of Mechanical Engineers, Part C: Journal of Mechanical Engineering Science, 0(0), 1-8.

Zeghloul, A., Messilem, A., Ghendour, N., Al-Sarkhi, A., Azzi, A., & Hasan, A. (2021). Theoretical study and experimental measurement of the gas liquid two-phase flow through a vertical Venturi meter. Proceedings of the Institution of Mechanical Engineers, Part C: Journal of Mechanical Engineering Science, 235(9), 1567-1584.